TA-105S

SENSITIVITY ANALYSIS OF THE RUNOFF IN THE LAND SURFACE MODELS FORCED BY THE OUTPUT OF MRI-AGCM 3.2 CLIMATE MODEL

Aulia Febianda Anwar Tinumbang
Department of Civil and Earth Resources Engineering Graduate School of Engineering
Kyoto University
Kyoto, Japan
anwar.febianda.28n@st.kyoto-u.ac.jp

Kazuaki Yorozu
Department of Civil and Earth Resources Engineering Graduate School of Engineering
Kyoto University
Kyoto, Japan

Yasuto Tachikawa
Department of Civil and Earth Resources Engineering Graduate School of Engineering
Kyoto University
Kyoto, Japan

Yutaka Ichikawa
Department of Civil and Earth Resources Engineering Graduate School of Engineering
Kyoto University
Kyoto, Japan

ABSTRACT
The risks of flooding in the future are projected to increase in magnitude and frequency under global warming. To make such projections, runoff output from general circulation models (GCMs) or regional climate models (RCMs) are widely used to simulate the river flow. Some studies have pointed out there are some gaps between the estimated discharge forced by the runoff from GCMs/RCMs and the observed discharge. In the GCMs/RCMs, runoff is estimated by the land surface model (LSM). To improve the accuracy of the simulated discharge forced by the runoff generated by LSM, it is necessary to figure out the sources of uncertainty in the model. Therefore, this study aims to is to conduct a sensitivity analysis of the runoff generated by two LSMs: SiBUC and MRI-SiB. This study utilized atmospheric data from the output of atmospheric general circulation model MRI-AGCM 3.2 as forcing in both LSMs. The numerical experiments were applied in the upper part of the Ping River Basin in Thailand, with the total catchment area is about 26,176 km^2. We found that even though the same forcing data forced both LSMs, the estimated runoff and its simulated discharge were different depending on the model. To figure out why such differences happened, different settings (e.g., parameters, structures) between the two models were examined. This study identified different settings that mainly affected the runoff generation and the simulated discharge in both LSMs. For example, incorporation of direct infiltration pathway from the soil surface into deeper soil layer in MRI-SiB caused a decrease of surface runoff and increase of subsurface runoff, consequently resulting in a slower response of the simulated discharge to the rainfall. It is thought that the findings in this study could provide some insights to identify the sources of uncertainty in LSMs and propose better settings for improving the runoff accuracy to reproduce the observed river flow.

Keywords— climate change; runoff; land surface models; river discharge

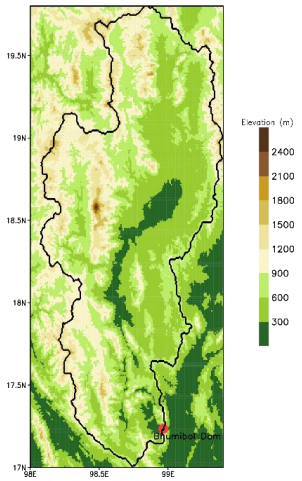

Fig. 1. Topography of upper part of Ping River. Black line shows basin boundary. Red circle shows Bhumibol Dam location.

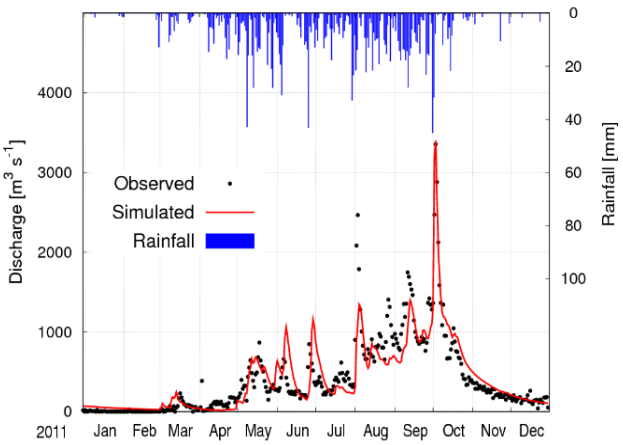

Fig. 2. Reproducibility of river discharge by SiBUC in 2011 at the outlet of Bhumibol Dam. Reproduced from Yorozu *et al*. (10).

INTRODUCTION

Many regions worldwide have been affected by unprecedented extreme floods and droughts in recent years. The latest assessment report by the Intergovernmental Panel on Climate Change (1) predicts that water-related disasters increase in magnitude and frequency owing to global warming. Previous impact assessment studies (2, 3) sought to project changes in future river discharge using runoff (ROF) output from general circulation models (GCMs) and regional climate models (RCMs). However, they pointed out that the simulated discharge by runoff from GCMs/RCMs is biased. This bias could be due to precipitation and/or runoff bias. The latter, ROF, is the focused in this study. The runoff is estimated using the land surface model (LSM) embedded in GCMs/RCMs. It is necessary to evaluate the performance of LSMs with respect to river discharge because runoff plays an essential role in river discharge simulation. In addition, it is important to identify sources of uncertainty in runoff generation processes in LSMs to enhance the model performance. In this study, we aimed to evaluate streamflow simulated by runoff from LSMs and investigate the sources of runoff uncertainty by analyzing the runoff generation schemes in the LSMs. Analysis of the sources of uncertainty in LSMs is necessary for improving the runoff accuracy to reproduce the observed river flow.

1 METHODOLOGY

1.1 Overview

In this study, two LSMs were utilized: Simple Biosphere including Urban Canopy (SiBUC) (4) and Meteorological Research Institute - Simple Biosphere Model (MRI-SiB) (5). Both LSMs have been developed based on Simple Biosphere (6). Therefore, the main functions are similar in both models. For example, soil water movement in both LSMs is described by three soil layers utilizing simplified Richards's equation. However, as the two of them have been developed independently, parameter settings, detailed model structures, etc., are different (described in section 1.3).

Numerical experiments for both LSMs were conducted in the upper part of the Ping River Basin in northern Thailand, as shown in Fig. 1. The basin is one of the main tributaries of the Chao Phraya River. The main dam in the basin is the Bhumibol Dam, which has a total catchment area of approximately 26,176 km^2.

In this study, both LSMs were forced by atmospheric data from MRI-AGCM 3.2S, a GCM with a mesh size of about 20 km (7). MRI-SiB is embedded in this climate model. SiBUC applied in this basin was developed by Yorozu et al. (8). They confirmed that the generated runoff by SiBUC could well reproduce the 2011-big flood event in this basin, as shown in Fig. 2, with Nash-Sutcliffe Efficiency (NSE) is 0.79, Root Mean Square Error (RMSE) is 219 m^3 s^{-1}, and the correlation coefficient is 0.90. Therefore, SiBUC was selected for this study.

Fig. 3 shows a framework of this study, which is divided into two parts: evaluation of discharge simulated by runoff from both LSMs, and investigation of runoff generation schemes in the LSMs.

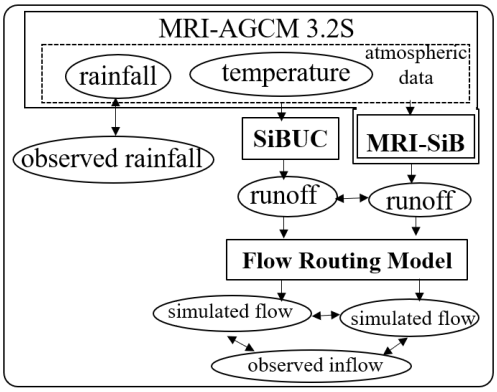

1. Evaluation of discharge simulated by LSMs.

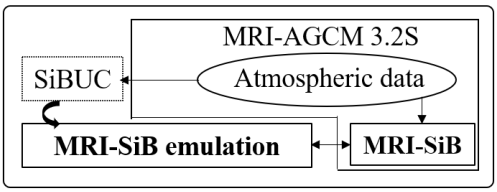

2. Investigation of runoff generation schemes in LSMs.

Fig. 3. Framework of this study.

1.2 Evaluation of discharge simulated by runoff from LSMs

First, we investigated the applicability of runoff generated by both LSMs to streamflow simulation. Before runoff simulation is performed, estimated rainfall by GCM was compared with observed historical data. In this study, CHIRPS (Climate Hazards Group InfraRed Precipitation with Station data) (9) rainfall dataset was selected as a reference. This dataset is a quasi-global satellite data product with in-situ station rainfall data. Observation data from rain gauges installed in this basin was not utilized in this study.

After the rainfall assessment, a runoff simulation was performed. We investigated the difference in water budget and runoff components by both SiBUC and MRI-SiB. Next, river flow was simulated by a flow routing model 1K-FRM (10) using the runoff from both LSMs. 1K-FRM is a distributed flow routing model developed based on a one-dimensional kinematic wave theory. The discharge simulated by both LSMs was evaluated with respect to observed inflow at the outlet of Bhumibol Dam. This study only utilized historical output data from MRI-AGCM 3.2S, consisting of 25 years from 1979-2003. Numerical simulations were performed for the whole 25 years. The first five-year results were discarded as model spin-up, and the last twenty years were used for analysis.

1.3 Investigation of runoff generation schemes in the LSMs

Past research has shown a considerable spread in runoff output among different LSMs (3, 11, 12). However, it is unclear whether this spread is related to parameters settings (i.e., soil parameters), model structures (i.e., infiltration mechanisms), or other reasons. Identifying uncertainty sources is challenging owing to the complexity of and different ways in which runoff generation schemes are described. To address such problems, we conducted sensitivity analysis which enabled us to investigate the effect of various settings on runoff estimation in LSMs.

Some different settings between the two LSMs are summarized in Table 1, based on the findings of our previous study (13). In both LSMs, land surface parameter settings (including soil and vegetation parameters) are different. For instance, soil parameters related to runoff and infiltration processes such as saturated hydraulic conductivity and saturated matric potential in MRI-SiB are higher than SiBUC. In contrast, soil depth in SiBUC is significantly deeper than in MRI-SiB. In addition, detailed model structures in both LSMs are also different. In MRI-SiB, there is a direct infiltration pathway into the second soil layer, which we called as "P_2 scheme" in this paper. Due to the incorporation of the P_2 scheme, when rainfall happens, some rainwater can infiltrate into the surface

TABLE 1 COMPARISON OF DIFFERENT SETTINGS BETWEEN SIBUC AND MRI-SIB

Settings	LSMs	
	SiBUC	**MRI-SiB**
Land surface parameters, for instance[a]: Saturated hydraulic conductivity, K_s (m s^{-1}) Saturated matric potential (m) Soil depth (m)	 1.44×10^{-6} -0.63 up to 12	 2×10^{-5} -0.086 up to 3.5
Direct infiltration pathway into a deeper soil layer	no	yes
Soil-water flow equation	Eq. (1a)	Eq. (1b)
Subsurface runoff equation	Eq. (2a)	Eq. (2b)

[a] based on dominant value

TABLE 2 EXPERIMENTAL DESIGNS

Experiments	Settings
1	Using MRI-SiB land surface parameters
2	MRI-SiB parameters and incorporating P_2 scheme
3	MRI-SiB parameters and neglecting gravitational drainage for calculating soil-water flow
4	MRI-SiB parameters and including hydraulic diffusion for estimating subsurface runoff
5	Combining all above settings

soil layer and directly into deeper soil layer. In SiBUC, such structure does not exist. The rainwater can only enter into the surface soil. Another difference is related to soil-water flow calculation. In SiBUC, soil-water flow between adjacent soil layers is based on Darcy's Law by considering hydraulic diffusion and gravitational drainage, as shown in Eq. (1a). In MRI-SiB, the gravitational drainage term is neglected, and it is only based on hydraulic diffusion, as indicated in Eq. (1b). Subsurface runoff calculation is also treated differently. SiBUC is based on gravitational drainage only, as indicated in Eq. (2a)., while in MRI-SiB, hydraulic diffusion is also considered, as shown in Eq. (2b).

$$Q_{i,i+1} = K\left[\frac{\partial \varphi}{\partial z} + 1\right] \quad (1a)$$

$$Q_{i,i+1} = K\left[\frac{\partial \varphi}{\partial z}\right] \quad (1b)$$

$$Q_3 = sin\emptyset_s K_s W_3^{2B+3} \quad (2a)$$

$$Q_3 = sin\emptyset_s K_s W_3^{2B+3} + \frac{\varphi_2 - \varphi_3}{z_3} \quad (2b)$$

note that $Q_{i,i+1}$ is soil-water flow between adjacent soil layer, K is hydraulic conductivity, K_s is saturated hydraulic conductivity, φ is matric potential, z is soil depth, Q_3 is subsurface runoff, $sin\emptyset_s$ is slope, W_i is soil wetness of i^{th} layer, and B is parameter.

In this study, sensitivity analysis was conducted to investigate the impact of different model settings on runoff estimation. The numerical experiments were performed by SiBUC by adopting MRI-SiB parameters and structures, and the results by MRI-SiB were set as a reference. In total, five experimental cases were conducted by SiBUC, as shown in Tabel 2. Experiment 1 was carried out to investigate the impact of different land surface parameters. Experiments 2 – 5 were conducted by changing land surface parameters and model structure. The impact of each setting was evaluated with respect to the change of runoff components (surface and subsurface runoff).

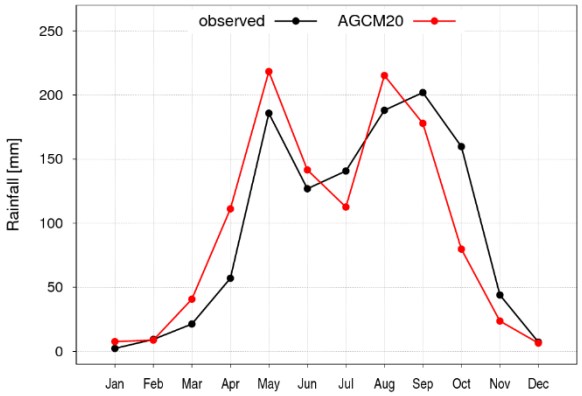

Fig. 4. Climatological mean of monthly rainfall

TABLE 3 COMPARISON OF WATER BUDGET COMPONENTS BETWEEN SiBUC AND MRI-SiB

Water budget components (mm year^{-1})	**LSMs**	
	SiBUC	**MRI-SiB**
Evapotranspiration (ET)	976	999
Runoff (ROF)	194	146
Surface runoff (Qs)	58	3
Subsurface runoff (Qsb)	136	143
Change of soil moisture (delSM)	-17	1

2 RESULTS: EVALUATION OF DISCHARGE SIMULATED BY LSMs

2.1 Assessment of rainfall output from MRI-AGCM 3.2S

Fig. 4 shows a comparison of 20-years-mean monthly rainfall from observation and simulation by GCM. Observed rainfall shows a distinct rainy season (from May to October) and dry season (from November to April). As seen, the GCM rainfall could capture the seasonal cycle of precipitation in this basin. The peak of observed rainfall is in September, while the GCM rainfall produces an earlier peak in August.

Basin average annual rainfall from GCM is close to the observation, which is 1144 mm. More than 80% of the annual rainfall occurs in the wet season, and the rest in the dry season. Simulated rainfall by GCM in the wet season slightly underestimates, while it overestimates the observed precipitation in the dry season.

2.2 Comparison of water budget components between LSMs

Table 3 shows 20-years-mean water budget components estimated by SiBUC and MRI-SiB. MRI-SiB tends to estimate higher evapotranspiration and lower runoff than that by SiBUC. In terms of runoff components, SiBUC predicts higher surface runoff and lower subsurface runoff than MRI-SiB. Surface runoff and subsurface runoff by SiBUC occupy about 30% and 70% of the total runoff, respectively. While, in MRI-SiB, subsurface runoff is dominant, and surface runoff only counts for 2% of the total runoff. This analysis has revealed the differences in water budget estimation and the ratio of runoff components between the two LSMs, even though they were forced with the same atmospheric forcing data. More detailed investigations to find out the reason for such differences are described in section 3.

2.3 Evaluation of streamflow simulated by runoff from LSMs

Before the streamflow simulated by both LSMs is evaluated, we examined characteristics of daily discharge by the two LSMs. Fig. 5 shows daily discharge estimated by SiBUC and MRI-SiB in 1991, as an example. In this figure, the observed discharge is not added as both of LSMs were forced by the output of the climate model, not the observation data. Both LSMs show different abilities in simulating the streamflow due to the differences in runoff estimation. As seen, simulated discharge

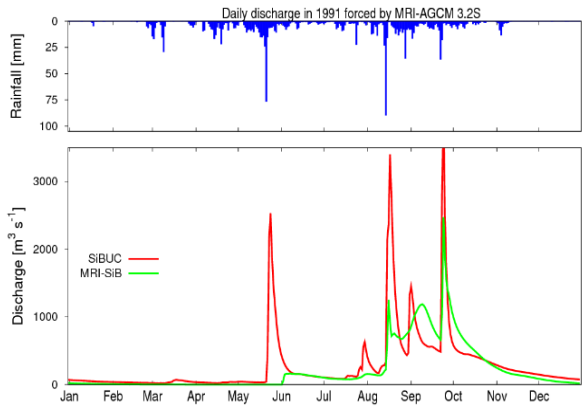

Fig. 5. Simulated daily discharge in 1991 by SiBUC (red line) and MRI-SiB (green line).

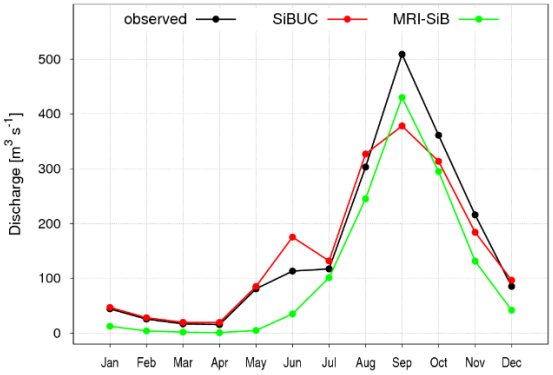

Fig. 6. Comparison of mean monthly streamflow between observed inflow (black line), simulated flow by SiBUC (red line) and MRI-SiB (green line).

by SiBUC tends to be higher than MRI-SiB, owing to higher runoff. The temporal pattern of increase and decrease of the hydrograph by SiBUC show a similar response to the rainfall events. The discharge by SiBUC, particularly in the case of heavy rainfall, was formed mainly through surface runoff. Consequently, it increases soon after the precipitation events. Meanwhile, the streamflow estimated by MRI-SiB does not show a high response, particularly at the beginning of rainfall events in May. As subsurface runoff is the dominant runoff component in MRI-SiB, the effect of catchment wetness is clear. During the transition between dry and wet seasons, the soil is in unsaturated condition. Therefore, the rainwater is first used to increase the soil moisture, and as the wetness of the soil gets higher, the discharge starts to rise.

Next, river flow simulated by runoff from both LSMs is evaluated by comparing climatological mean (20-years-mean) of monthly simulated and observed river flow, as shown in Fig. 6. Streamflow estimated by SiBUC shows a similar time series of observed discharge: low flow in the dry season, slightly high flow in the early rainy season (May to July), and high flow in the late rainy season (August to October). On the other hand, peak discharge by MRI-SiB is closer than SiBUC to the peak observation. However, the discharge by MRI-SiB failed to reproduce the observed discharge, particularly in the early wet season. That is due to the difference in runoff estimation by both LSMs, as mentioned earlier. In terms of volume, simulated streamflow by SiBUC in both wet and dry seasons is close to the observed river flow. Meanwhile, the discharge by MRI-SiB underpredicts the observation throughout the year.

This study has revealed the different runoff estimations by each LSM and how it affects the simulated streamflow.

3 INVESTIGATION OF RUNOFF GENERATION SCHEMES in LSMs

Fig. 7 shows changes in runoff components by adopting MRI-SiB settings in SiBUC. As mentioned previously, both LSMs show a significant difference in the ratio of runoff components: SiBUC tends to estimate higher surface runoff and lower subsurface runoff than MRI-SiB. In contrast, in MRI-SiB, subsurface runoff is the dominant runoff component. That difference is owing to different settings among both LSMs.

First, the impact of land surface parameters is investigated in experiment 1. By adopting MRI-SiB soil parameters in SiBUC, surface runoff significantly increases, while subsurface runoff decreases compared to SiBUC results. That could be due to the shallow soil depth setting in the MRI-SiB. Thinner soil depth could increase the surface runoff since the soil has a lower capacity to store the rainwater.

Next, the impact of incorporating the P_2 scheme is analyzed in experiment 2. As seen, surface runoff decreases and subsurface increases compare to experiment 1. The surface runoff reduces due to an increase of infiltrated rainwater in the soil. As the infiltrated water increases, the subsurface runoff also becomes higher.

Impact of neglecting gravitational drainage in Darcy's Law is shown in experiment 3. Surface runoff is significantly lower compared to experiment 1. Ignoring gravitational drainage might cause lower

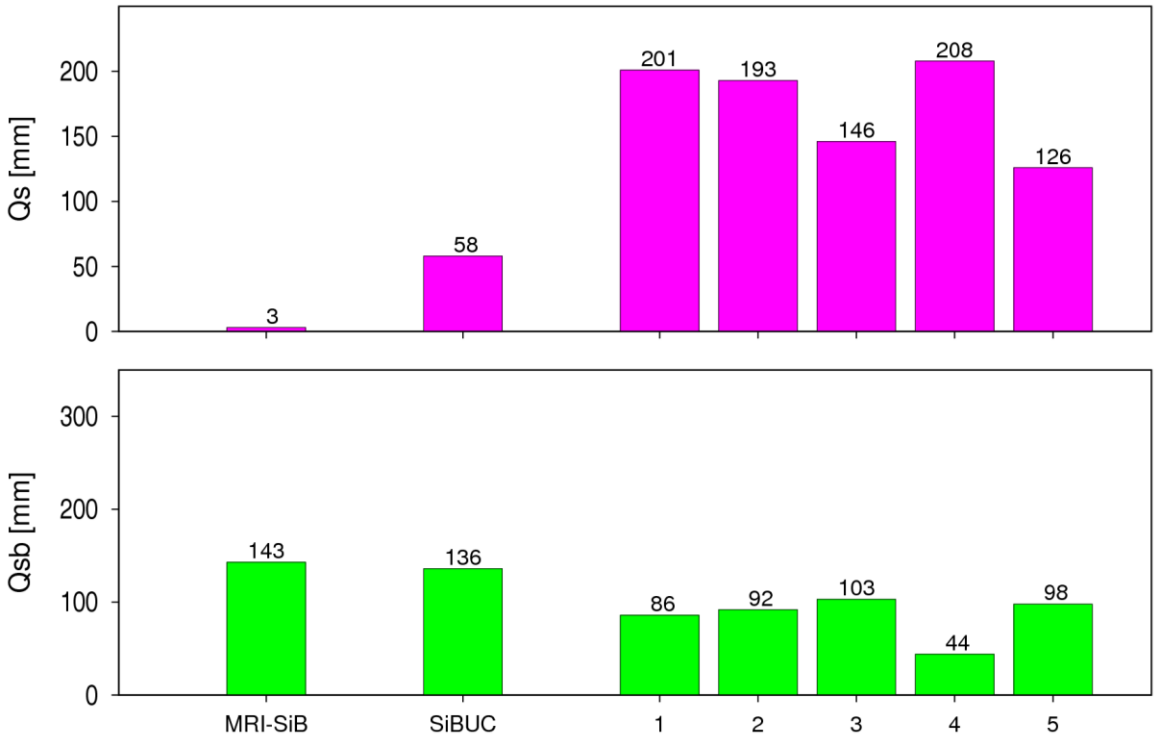

Fig. 7. Results of sensitivity analysis to investigate the impacts of different settings among LSMs. Pink and green bars represent surface runoff (Qs) and subsurface runoff (Qsb), respectively.

soil-water flow. As a result, soil moisture was kept high, resulting in higher evapotranspiration and lower runoff.

Experiment 4 analyzed the impact of considering hydraulic diffusion on subsurface runoff estimation. The increase or decrease of subsurface runoff depends on the soil moisture of the second and third soil layers. If the soil moisture of the second layer is higher than the third layer, subsurface runoff increases; otherwise, it decreases. This analysis shows that considering hydraulic diffusion for subsurface runoff estimation results in the lower subsurface runoff compared to experiment 1.

In experiment 5, all model parameters and structures of MRI-SiB were adopted in SiBUC. Surface runoff is higher, and subsurface runoff is lower than experiment 1, owing to the impact of each setting, as already mentioned earlier.

Even though SiBUC has adopted all MRI-SiB settings, the runoff characteristics of MRI-SiB still could not be well reproduced. Therefore, further investigation is necessary to understand which other settings affect the runoff estimation by LSMs. Throughout this activity, we have demonstrated a framework to identify sources of bias in the runoff generation schemes in the LSMs. This framework can be extended to propose better settings for improving the runoff accuracy by LSMs to reproduce the observed river flow.

4 SUMMARY

This research investigated the applicability of runoff generated by two land surface models (LSMs): SiBUC and MRI-SiB, for streamflow simulation. Atmospheric output from MRI-AGCM 3.2S was used as forcing for both LSMs. Based on water budget analysis, SiBUC tended to estimate higher evapotranspiration and lower runoff than MRI-SiB. Different LSMs also generated different runoff characteristics. SiBUC estimated higher surface runoff and lower subsurface runoff than MRI-SiB. In comparison, the subsurface runoff was the dominant runoff component in MRI-SiB. The different runoff estimation by each LSM has impacts on the simulated streamflow. To determine the reasons for such differences, runoff generation schemes in both LSMs were analyzed in detail. This study has shown some different settings that contribute to the sources of runoff uncertainty in both LSMs. However, further work is necessary to identify which other settings affect the runoff estimation by LSMs.

ACKNOWLEDGMENTS

This study is supported by the Integrated Research Program for Advancing Climate Models (TOUGOU) Theme-C and D supported from MEXT Japan (Grant Number JPMXD0717935561 and JPMXD0717935498).

REFERENCES

(1) IPCC (2021): Climate Change 2021: The Physical Science Basis. Contribution of Working Group I to the Sixth Assessment Report of the Intergovernmental Panel on Climate Change [Masson-Delmotte, V., P. Zhai, A. Pirani, S.L. Connors, C. Péan, S. Berger, N. Caud, Y. Chen, L. Goldfarb, M.I. Gomis, M. Huang, K. Leitzell, E. Lonnoy, J.B.R. Matthews, T.K. Maycock, T. Waterfield, O. Yelekçi, R. Yu, and B. Zhou (eds.)]. *Cambridge University Press*. In Press.

(2) Hirabayashi, Y., Mahendran, R., Koirala, S., Konoshima, L., Yamazaki, D., Watanabe, S., Kim, H., and Kanae, S. (2013): Global flood risk under climate change, *Nature Climate Change*, Vol. 3, pp. 816-821.

(3) Nohara, D., Kitoh, A., Hosaka, M., Oki, T. (2006): Impact of Climate Change on River Discharge Projected by Multimodel Ensemble, *J. Hydrometeorol.*, Vol. 7, pp. 1076–1089.

(4) Tanaka, K. (2005): Development of the new land surface scheme SiBUC commonly applicable to basin water management and numerical weather prediction model, *doctoral dissertation*, Kyoto University.

(5) Hirai, M., Sakashita, T., Kitagawa, H., Tsuyuki, T., Hosaka, M., Oh'izumi, M. (2007): Development and Validation of a New Land Surface Model for JMA's Operational Global Model Using the CEOP Observation Dataset, *J. Meteor. Soc. Jpn.*, Vol. 85A, pp. 1-24.

(6) Sellers, P. J., Mintz, Y., Sud, Y. C., and Dalcher, A. (1986): A simple biosphere model (SiB) for use within general circulation models, *J. Atmos. Sci.*, Vol. 43, No. 6, pp. 505-531.

(7) Mizuta, R., Yoshimura, H., Murakami, H., Matsueda, M. Endo, H., Ose, T., Kamiguchi, K., Hosaka, M., Sugi, M. Yukimoto, S., Kusunoki, S.,and Kitoh, A. (2012): Climate simulations using MRI-AGCM 3.2 with 20-km grid, *J. Meteor. Soc. Jpn.*, Vol. 90A, pp. 233-258.

(8) Yorozu, K., Kurosaki, N., Ichikawa, Y., Kim, S., and Tachikawa, Y., (2018): A study on long-term river discharge data generation by distributed hydrologic model and recombination atmospheric data, *J. JSCE*, Ser. B1 (Hydraulic Engineering), Vol. 74, pp. I_127-I_132 (in Japanese).

(9) Funk, C., Peterson, P., Landsfeld, M., Pedreros, D., Verdin, J., Shukla, S., Husak, G., Rowland, J., Harrison, L., Hoell, A., and Michaelsen, J. (2015): The climate hazards infrared precipitation with stations-a new environmental record for monitoring extremes, *Scientific Data 2*, 150066.

(10) Kyoto University Department of Civil and Earth Resources Engineering Hydrology and Water Resources Research Laboratory: 1K-FRM/1K-DHM, http://hywr.kuciv.kyoto-u.ac.jp/products/1K-DHM/1K-DHM.html [Access: November 24, 2021].

(11) Tinumbang, A. F. A., Yorozu, K., Tachikawa, Y., Ichikawa, Y., Sasaki, H., Nakaegawa, T. (2019): Analysis of runoff characteristics generated by land surface models and their impacts on river discharge, *J. JSCE*, Ser. B1 (Hydraulic Engineering), Vol. 75, No. 2, pp. I_127-I_276.

(12) Falloon, P., Betts, R., Wiltshire, A., Dankers, R., Mathison, C., McNeall, D., Bates, P., and Trigg, M. (2011): Validation of river flows in HadGEM1 and HadCM3 with the TRIP river flow model, *J. Hydrometeorol.,* Vol. 12, No. 6, pp. 1157-1180.

(13) Tinumbang, A. F. A., Yorozu, K., Tachikawa, Y., Ichikawa, Y., Sasaki, H., Nakaegawa, T. (2020): Impacts of model structures and soil parameters on runoff characteristics in land surface models, *J. JSCE*, Ser. B1 (Hydraulic Engineering), Vol. 76, No. 2, pp. I_217-I_222.